RWTH AACHEN

RHEINISCH-WESTFÄLISCHE TECHNISCHE HOCHSCHULE AACHEN

Institut für Mathematik

Lead-Lag Relationship using a
Stop-and-Reverse-MinMax Process

by

S. Maier-Paape
A. Platen

Report No. **79** 2015

April 2015

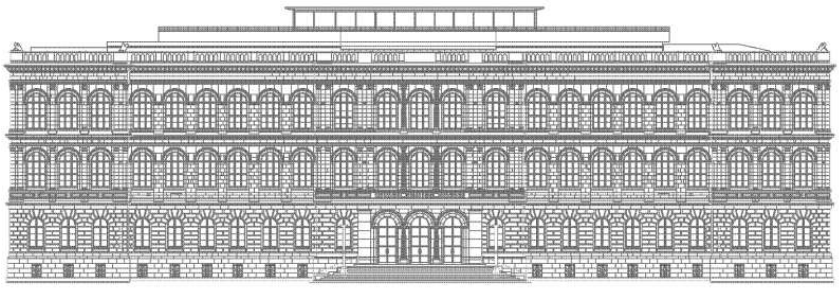

Institute for Mathematics, RWTH Aachen University

Templergraben 55, D-52062 Aachen
Germany

Lead-Lag Relationship using a Stop-and-Reverse-MinMax Process

Stanislaus Maier-Paape
Institut für Mathematik, RWTH Aachen,
Templergraben 55, D-52052 Aachen, Germany
maier@instmath.rwth-aachen.de

Andreas Platen
Institut für Mathematik, RWTH Aachen,
Templergraben 55, D-52052 Aachen, Germany
platen@instmath.rwth-aachen.de

April 24, 2015

Abstract The intermarket analysis, in particular the lead-lag relationship, plays an important role within financial markets. Therefore a mathematical approach to be able to find interrelations between the price development of two different financial underlyings is developed in this paper. Computing the differences of the relative positions of relevant local extrema of two charts, i.e., the local phase shifts of these underlyings, gives us an empirical distribution on the unit circle. With the aid of directional statistics such angular distributions are studied for many pairs of markets. It is shown that there are several very strongly correlated underlyings in the field of foreign exchange, commodities and indexes. In some cases one of the two underlyings is significantly ahead with respect to the relevant local extrema, i.e., there is a phase shift unequal to zero between these two underlyings.

Keywords lead-lag relationship, intermarket analysis, local extrema, empirical distribution

1 Introduction

It is well-known that financial markets can be strongly correlated in such a way that their market values show a similar behavior. Knowing the exact connection between two markets would be very helpful for risk-averse investment strategies. In case that two markets are perfectly correlated it would make no difference to invest in either one of them or both together. One simply cannot diversify the risk on both markets. In case it is known that one market leads the other, one is able to use the leading market as an indicator to predict the price development of the other market. Knowing this connection between the two markets can be useful to improve the investment strategy. Therefore we develop a method for quantizing the interrelation of two markets from a different point of view: We want to be able to identify a possible phase shift between two markets if they are correlated.

This subject has been approached in a variety of articles. One approach is to decompose the time series of two markets on a scale-by-scale basis into components with different frequencies using wavelets. The lead-lag relationship is studied by comparing the components of one selected level of the wavelet transformation for two markets, see e.g. [5, 10, 14, 16, 21, 22]. More on wavelet methods in finance can be found in the book of Gençay, Selçuk and Whitcher [13].

Other methods working with correlation, auto-correlation and similar quantities can be found e.g. in [4, 6, 7, 9, 12, 15, 24]. Didier, Love and Pería [8] studied the comovements during 2007–2008 crisis. A different but related topic is the lead-lag relationship between news, e.g. on Twitter, and stock prices, see e.g. [3, 18].

For the intermarket analysis from a point of view of the technical analysis see e.g. the book of Murphy [20] and also of Ruggiero [23].

However, to the best of the author's knowledge, the approaches found in the literature do not follow a geometric approach, e.g. they do not take local extreme values of the time series into account. Decomposing the time series using wavelets permits to write the time series as the sum of wavelike components with different frequency spectrum. Using these components for comparison of different markets will therefore compare only parts of the original time series. The problem is that these components can be hidden in the original time series such that a possible lag observed between the components of the same level does not necessarily mean that this lag can be observed in the time series itself, e.g. by comparing reversal points. Therefore it is not clear how to interpret the results with regards to an application.

Since we want to be able to receive results giving us an observable lead-lag relationship of two time series, we prefer a geometrical approach. For this reason we need significant points to be able to uniquely identify a lead or lag if any. Very important situations are reversal points and thus the points in time of relevant local extreme values which represents the moment of reversal. A possible lead or lag can then directly be seen by comparing the local extrema of both charts. Such an ansatz could be used for trading these financial products and offers a deep insight into the lead-lag relationship between two markets because an empirical distribution over all local phase shifts can be identified. Additionally the results are not hidden in just one single value like cross-correlation.

The paper is organized as follows: The search for the relevant local extreme values is far from being unique. Therefore we discuss in Section 2 the approach to find these extreme values for a given pair of markets which we want to compare. Using these values we can compute local phase shifts of both markets which gives us a corresponding empirical distribution. To analyze the results we introduce the directional statistics in Section 3. Now we can apply our approach to historical data, e.g. for foreign exchange, commodities and indexes, which we do in Section 4. In Section 5 we give some conclusions.

2 Method for intermarket analysis

Suppose we want to compare two financial underlyings namely market A and market B for lead and lag. First we take one chart for each underlying with the same bar size, e.g. a 60 min chart, depending on our interest. Now we want to decide whether these two charts are correlated and show lead or lag. Of course if both underlyings are fully uncorrelated we cannot compare them. Therefore let us assume that there is a connection between these two charts.

Since we prefer a geometrical ansatz we need the points in time of relevant local extreme values. If each maximum occurs for both charts at the exact same time and the same holds true for the minimal values we can say that both underlyings run perfectly synchronous. If the maximum of chart B occurs shortly after the maximum of chart A, we observe that market B has a lag compared to market A.

Such a comparison could easily be done by hand in a very intuitive way. If one compares two markets and gets a feeling for lead-lag relationship, e.g. assume market A leads B, one directly benefits from this knowledge because right after a reversal point in market A would most likely occur a reversal point in market B. This can be very useful for several strategies (for position entries and also for exits).

Of course doing an extensive study by hand would be very time consuming and not objective. For an automatic approach we first need an appropriate method to identify local extrema for both time series. The MinMax algorithm introduced by Maier-Paape [17] is a method which yields such a series of alternating relevant local extrema (called MinMax process) and will therefore be used in the following. This method uses a so called SAR (stop and reverse) process to identify up and down movements. If an up movement is detected the MinMax algorithm searches for a maximum and fixes this local maximal value if the movement phase reverses to a down movement. Minimal values are searched during down movement phases. The underlying SAR process could be the MACD (moving average convergence/divergence) indicator of [1] which, simplified speaking, indicates an up movement if the MACD series lies above its signal line and a down movement when its vice versa. See [17] for the details.

The SAR process controls the frequency of detected local extreme values and, in general, is controlled by some parameters (default for MACD are 12, 26 and 9). In this paper we will always use the MACD as SAR process. Instead of adjusting several parameters separately we use just a common factor, called timescale, that scales the three default parameters at the same time. Increasing the timescale leads to less extreme values while decreasing timescale leads to more extreme values, i.e. a finer resolution.

Note that the MACD series can oscillate quickly around the signal line which leads to many small and insignificant local extreme values. To avoid this problem we require for a change of the direction of the SAR process that the distance of MACD and its signal line needs to exceed some minimal threshold of $\delta = 0.3 \cdot \mathrm{ATR}(100)$, where ATR means the average true range, see [17, Subsection 2.1] for the details.

From now on we use this MinMax algorithm because this is a very flexible tool to identify local extreme values. As far as we know this method is the only one which identifies local extreme values exactly and is continuously adjustable. Since a financial time series always has some noise there is no unique objective choice for relevant local extrema of a financial time series. Therefore this process needs to be parameter dependent to adjust the resolution of the minima and maxima.

One question is how to choose the "right" parameter. This will be discussed at the end of this section. For the moment let us assume we already found "good" parameters for market A. The MinMax process then yields consecutive minima and maxima denoted by $(t_i, X_i)_{i=1,\dots,N}$ with points in time $t_1 \leq \dots \leq t_N$ and consecutive price values X_i. To be able to compare these points, we measure the time in seconds since 1st January 1970. For this wavelike time series we can compute the mean wavelength by

$$\lambda := \frac{1}{N-1} \sum_{i=1}^{N-1} 2(t_{i+1} - t_i) = 2\frac{t_N - t_1}{N-1}. \tag{1}$$

Note that λ depends on the parameters used in the MinMax algorithm since the minima and maxima depend on the used parameters.

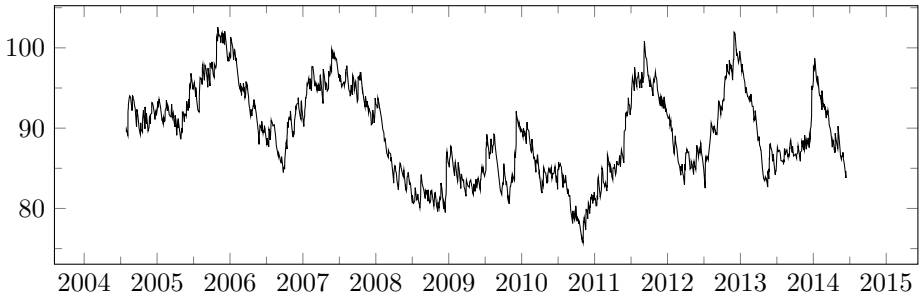

Figure 1: Moving average of wavelengths over $N-1=49$ cycles for S&P 500 on a 60 min chart.

Fixing these parameters for the second market gives us the extreme values $(\tilde{t}_i, \tilde{X}_i)_{i=1,...,\tilde{N}}$ with mean wavelength $\tilde{\lambda}$. Of course it makes no sense to compare both markets using these extreme values for very different wavelengths λ and $\tilde{\lambda}$. Therefore we fit the parameters of the MinMax process for market B so that $\tilde{\lambda} = \lambda$ holds true.

Remark 1. *Note that in general we can not expect a constant but only a time dependent wavelength which can vary a lot, see Figure 1, where the moving average of wavelengths over* $N-1=49$ *cycles is shown, i.e.* $\frac{1}{49}\sum_{i=s-49}^{s-1} 2(t_{i+1}-t_i)$ *where* s *is the current time index. Therefore matching the mean wavelength for both markets means just matching the level of refinement and not the position of the extreme values themselves.*

Since we are interested in the lead-lag relationship between market A and B we only need to find the relationship of points in time of the extrema by finding the relative positions of $(\tilde{t}_i)_{i=1,...,\tilde{N}}$ within $(t_j)_{j=1,...,N}$. In this case we call market A the primary market and market B the secondary market. The overall procedure is as follows:

1. Fix the desired mean wavelength $\lambda^* > 0$.
2. Find all local extreme values $(t_i, X_i)_{i=1,...,N}$ and $(\tilde{t}_j, \tilde{X}_j)_{j=1,...,\tilde{N}}$ for the primary and the secondary market, respectively, such that the mean wavelengths (1) for both markets on the full data base matches λ^*, i.e. that we have $2\frac{t_N - t_1}{N-1} \approx \lambda^* \approx 2\frac{\tilde{t}_{\tilde{N}} - \tilde{t}_1}{\tilde{N}-1}$.
3. Find $j_1, j_2 \in \{1, ..., \tilde{N}\}$ such that $\tilde{t}_{j_1} = \min\{\tilde{t}_j : \tilde{t}_j \geq t_1\}$ and $\tilde{t}_{j_2} = \max\{\tilde{t}_j : \tilde{t}_j < t_N\}$. For each $j \in \{j_1, ..., j_2\}$ do the following:
   a) Find $i \in \{1, ..., N-1\}$ such that $t_i \leq \tilde{t}_j < t_{i+1}$.
   b) Define the phase shift of extreme value $(\tilde{t}_j, \tilde{X}_j)$ regarding the extreme values (t_i, X_i) and (t_{i+1}, X_{i+1}). Here we use the linear relative distance between the corresponding extrema values measured as an angle. We set

$$\alpha_j^{\lambda^*} := \frac{\tilde{t}_j - s_j}{t_{i+1} - t_i} \cdot \pi \in [-\pi, \pi), \tag{2}$$

   where

$$s_j := \begin{cases} t_i, & \text{if } X_i \text{ and } \tilde{X}_j \text{ are both maxima or both minima,} \\ t_{i+1}, & \text{if } X_{i+1} \text{ and } \tilde{X}_j \text{ are both maxima or both minima.} \end{cases} \tag{3}$$

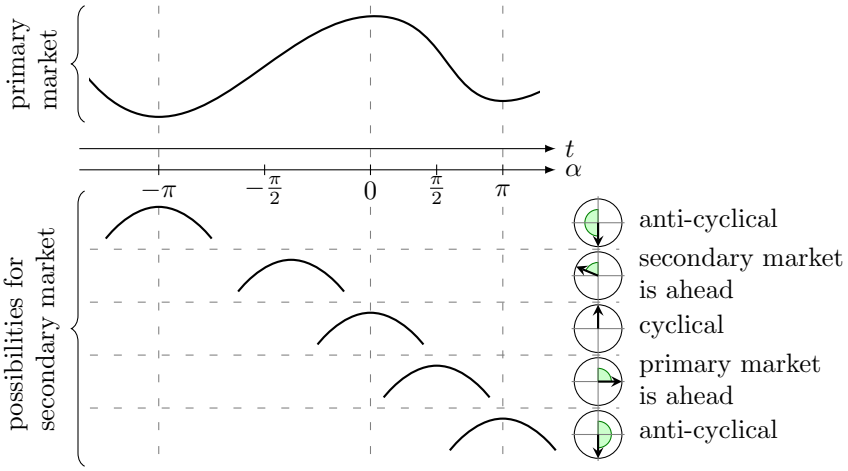

Figure 2: Computation of α in (2).

Figure 2 shows some examples for the position of a maximum of the secondary market relative to some extreme values of the primary market.

4. We end up with the empirical circular distribution $(\alpha_j^{\lambda^*})_{j=j_1,\dots,j_2} \subset [-\pi, \pi)$ depending on the mean wavelength λ^*.

Negative α resemble a front-running (lead) of the secondary market, positive α resemble a time lag of the secondary market. The result can be interpreted on the unit sphere $S^1 = \{(\sin\alpha, \cos\alpha) \in \mathbb{R}^2 : \alpha \in [-\pi, \pi)\}$ and gives us all observations of local phase shifts between two markets.

Remark 2. *This approach is independent of the openings of the stock exchange for market A and market B. Since we measure the points in time t_i and $\tilde{t}_j$ in seconds since 1st January 1970 we just put these values into* (2) *and the machinery works straight forward.*

Remark 3. *The above method has only one parameter, namely the mean wavelength λ^*, see step 1. Therefore we can compute different distributions for different wavelengths. It turns out that the results in most cases do not depend on the wavelength. Therefore we compute $(\alpha_i^{\lambda})_{i=1,\dots,n(\lambda)}$ for many values of the mean wavelength λ. For each λ we can generate a histogram or rather a bar plot and at the end we can compute the average of all bars including standard deviation.*

Remark 4. *Note that the extreme values cannot be determined in real time. There is always at least a small time lag. Therefore we can also identify such an empirical distribution if we use the point in time when the extreme value is confirmed by the MinMax algorithm instead of the point in time of the extreme value itself.*

3 Directional statistics

Since we work with circular distributions, the mean and variance must be computed in an appropriate way, see e.g. [11, 19]. This can be used to identify a possible phase shift. We

introduce the basic statistical quantities in Subsection 3.1. For a deeper analysis we list some interesting statistical tests in Subsection 3.2 and give an approximation of the lead or lag in Subsection 3.3.

3.1 Basic quantities

Now we will discuss how to calculate estimators, e.g. for the mean angular direction. Details on computations for a general distribution with a 2π periodic probability density function f can be found in [11, Section 3.2].

The first step is to identify the angles by vectors on the unit sphere S^1. Let $(\alpha_j)_{j=1,...,N} \subset [-\pi, \pi)$ be the outcomes of a discrete distribution for the phase shift of two markets of interest. We can identify each angle α_j with a point on the unit sphere

$$\mathbf{r}_j := \begin{pmatrix} \sin \alpha_j \\ \cos \alpha_j \end{pmatrix} \in S^1$$

for $j = 1, ..., N$. In this two-dimensional space we can compute the *mean resultant vector* which is defined by

$$\hat{\mathbf{r}} := \frac{1}{N} \sum_{j=1}^{N} \mathbf{r}_j.$$

Note that for the length of $\hat{\mathbf{r}}$ we have $\|\hat{\mathbf{r}}\|_2 \leq 1$ because it is a convex combination of vectors in S^1. If $\hat{\mathbf{r}} \neq 0$ choose the *mean angular direction* $\hat{\alpha} \in [-\pi, \pi)$ such that

$$\begin{pmatrix} \sin \hat{\alpha} \\ \cos \hat{\alpha} \end{pmatrix} = \frac{1}{\|\hat{\mathbf{r}}\|_2} \hat{\mathbf{r}}. \tag{4}$$

Of course $\hat{\mathbf{r}}$ could be zero and thus no unique mean angular direction would exist. This is the case, e.g., if the angles are uniformly distributed all around S^1. If this is the case for the phase shifts between two markets then there is no connection between them and the analysis of the results would already be finished. Since we are interested in at least slightly correlated markets we do not expect this behavior.

Nevertheless even in the case where $\|\hat{\mathbf{r}}\|_2 > 0$, the length of $\hat{\mathbf{r}}$ could be small. This happens if the outcomes of the distribution have a large variance. In contrast a length of $\hat{\mathbf{r}}$ near 1 indicates a small variance and a high concentration of the outcomes near to its mean angular direction. Therefore we need to consider the *circular variance* (cf. [11, Section 2.3.1, Equation (2.11)]) which can be defined by

$$\hat{S} := 1 - \|\hat{\mathbf{r}}\|_2 \in [0, 1].$$

To be able to also measure the skewness and the peakedness we define the *circular skewness* by

$$\hat{b} := \frac{1}{N} \sum_{j=1}^{N} \sin(2(\alpha_j - \hat{\alpha})) \in [-1, 1]$$

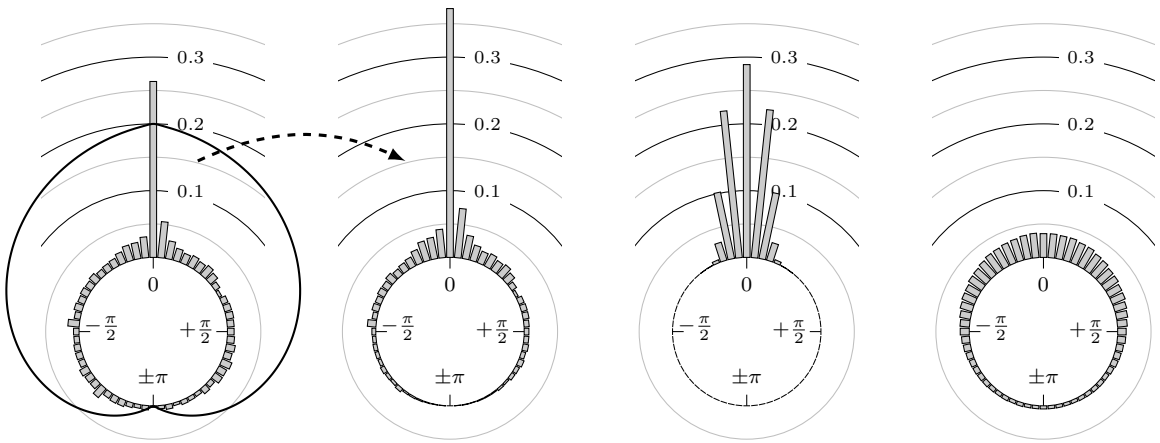

Figure 3: First: Example of a possible distribution of phase shifts and a hat function on S^1; Second: Corresponding weighted version of the example distribution from first plot; Third: Plot of the probability density functions of von Mises distributions mean location parameter $\mu = 0$ and concentration parameters $\kappa = 50$; Fourth: Same as third but with $\kappa = 1$.

and the *circular kurtosis* by

$$\hat{k} := \frac{1}{N}\sum_{j=1}^{N}\cos(2(\alpha_j - \hat{\alpha})) \in [-1, 1].$$

Since we are interested in the possible lead or lag between two markets we want to reduce the influence of outliers which are far away from the mean angular direction. For this reason we use a hat function on S^1 to weight the empirical distribution with the hat near the position of the highest peak of the distribution. Then all reasonable data near the peak get high weights and thus more influence in our statistics, while less important data, i.e. the outliers, obtain small weights. We expect that the peaks of the distributions are near zero up to some lead or lag, i.e. the two markets are positive correlated. Therefore we use the hat function which has its hat (maximum) at zero and is zero (minimum) at $\pm\pi$. The first two plots of Figure 3 show an example for an observed distribution and its weighted counterpart, respectively. From the weighted distribution we can compute the *weighted mean angular direction* $\hat{\alpha}^{(w)}$ as in (4).

3.2 Statistical tests

Most of the statistical tests require an underlying von Mises distribution, see e.g. [11, Section 3.3.6], which is often used as an analogon to normal distribution on the unit sphere. The distribution we get for our application is not exactly a von Mises distribution but has a similar shape, see Figure 3. In this figure the distribution of phase shifts has a similar shape to two superposed von Mises distribution, one with a large and one with a small concentration parameter κ. Thus it is possible, that the phase shifts correspond to a von Mises distribution plus noise, e.g. white noise. Nevertheless we use the following statistical

tests in order to be able to classify the results even if they are designed for von Mises distributions.

Since we do not know the underlying distribution for the phase shifts we only get some realizations. Computing the quantities in Section 3.1 using the formulas by putting in our observations will give us the estimators which will be denoted by $\hat{\alpha}$, $\hat{\alpha}^{(w)}$, $\hat{S}$, $\hat{b}$ and $\hat{k}$, respectively.

Next we want to verify the quality of our mean angular direction. Therefore we compute the $(1-\delta)\%$-confidence intervals for the population mean, such that $L_1 := \hat{\alpha} - d$ and $L_2 := \hat{\alpha} + d$ are the lower and upper confidence limits of the mean angular direction, respectively, see [25, Section 26.7]. For the weighted mean $\hat{\alpha}^{(w)}$ we denote the confidence interval by $d^{(w)}$. We always use $\delta = 5\,\%$.

To test for zero mean which would imply that there is no lead or lag relationship we can perform the one sample test for mean angle, which is similar to the one sample t-test on a linear scale. Let $\alpha_0 \in [-\pi, \pi)$ be the mean angular direction for which we want to test and $\bar{\alpha}$ the mean angular direction of the underlying (unknown) distribution. We test for

$$H_0 : \bar{\alpha} = \alpha_0,$$
$$H_1 : \bar{\alpha} \neq \alpha_0$$

by checking whether $\alpha_0 \in [L_1, L_2]$ using our estimator $\hat{\alpha}$ and its $95\,\%$ confidence interval, see [25, Section 27.1 (c)]. In our case we will set $\alpha_0 = 0$. The result of this test is then given by

$$h_m := \begin{cases} 0, & \text{if } H_0 \text{ can not be rejected, i.e. } \alpha_0 = 0 \in [L_1, L_2], \\ 1, & \text{otherwise.} \end{cases}$$

In Remark 3 we noted that we will generate empirical distributions for different mean wavelengths, say $n \in \mathbb{N}$ different values. To compare all these distributions for the same pair of markets we can use the one-factor ANOVA or Watson-Williams test (multi-sample test). It assesses the question whether the mean directions of two or more groups are identical or not, i.e. it tests for

H_0 : All of n groups share a common mean direction, i.e., $\bar{\alpha}^{(1)} = ... = \bar{\alpha}^{(n)}$.

H_1 : Not all groups have a common mean direction,

see [25, Section 27.4 (b)]. The output of this test is a p-value, i.e. the probability of getting results which are at least as extreme as our observation assuming the null hypothesis is true. Thus a large p-value indicates that the null hypothesis holds true. We denote this value by $p_{ww} \in [0, 1]$.

3.3 Lead or lag

Using the mean angular direction $\hat{\alpha}$ and its confidence interval we can roughly approximate the lead or lag. Assume we have a mean wavelength of 100 candles on a 60 min chart. The mean wavelength would then be approximately $60\,\text{min} \cdot 100 = 6000\,\text{min}$. This value equates 2π. Thus the mean of the lead or lag ℓ can be approximated by

$$\ell \approx \frac{\hat{\alpha}}{2\pi} \cdot 6000\,\text{min}$$

and the corresponding confidence interval is approximated by $[\ell - d_\ell, \ell + d_\ell]$ where

$$d_\ell \approx \frac{d}{2\pi} \cdot 6000\,\text{min}.$$

Analogously we can compute the lead or lag using the weighted mean angular direction which we denote by $\ell^{(w)}$ and $d_\ell^{(w)}$, respectively, i.e. $\ell^{(w)} \approx \frac{\hat{\alpha}^{(w)}}{2\pi} \cdot 6000\,\text{min}$ and $d_\ell^{(w)} \approx \frac{d^{(w)}}{2\pi} \cdot 6000\,\text{min}$. Note that a positive value for ℓ and $\ell^{(w)}$ means that the primary market leads the secondary and vice versa for a negative value.

To answer the question which market is ahead, if any, we make the following definition.

Definition 1. *For positive correlated markets, i.e.* $|\hat{\alpha}^{(w)}| \leq \frac{\pi}{2}$*, we say* one market leads the other *if* $\hat{\alpha}^{(w)}$ *is significantly different from zero, i.e.*

$$\begin{aligned} &\textit{if } \ \hat{\alpha}^{(w)} - d^{(w)} > 0 \quad \rightsquigarrow \quad \textit{primary market leads,} \\ &\textit{if } \ \hat{\alpha}^{(w)} + d^{(w)} < 0 \quad \rightsquigarrow \quad \textit{secondary market leads.} \end{aligned}$$

4 Empirical study

Now we study different markets from commodities to foreign exchanges. In Subsection 4.1 we explain the setting and give some details on the choice of parameters. The angular histograms and the statistical results are then shown in Subsection 4.2.

4.1 Settings

In this paper we focus on the 60 min chart. The wavelengths we use to adjust the MinMax process for the primary market, see Remark 3, are of size of 30 candles up to 180 candles. For the Watson-Williams test, see Section 3.2, this leads to $n = 151$ groups.

Since we have given the wavelength in number of candles we proceed as follows to "synchronize" the markets:

1. Choose the desired mean wavelength $\lambda^*_{\text{candles}} \in \{30, 31, ..., 180\}$ in number of candles.
2. Adjust the parameter for the MinMax process on the primary market, such that the wavelength of the primary market in number of candles, ignoring the time when the stock exchange is closed, matches $\lambda^*_{\text{candles}}$.
3. Calculate the corresponding wavelength λ^* in seconds for the primary market, this time considering the time when stock exchange is closed.
4. Adjust the MinMax process on the secondary market, such that the wavelength of the secondary market in seconds matches λ^*, i.e. perform step 2 from Section 2, where the primary market is already fixed.
5. Proceed with steps 3 and 4 from Section 2.

For most computations of the directional statistics the MATLAB library CircStat [2] has been used and all angles are measured in radian.

The markets which we examine including the period of time for the available candle data are listed in Table 1. Note that the start date is not the same for all markets. If we examine a combination of markets with different initial dates we use the smaller period of time for both markets.

market	underlying	initial date
Eurex DAX	DAX Futures	December 10, 2003
Eurex BUND	Euro-Bund Futures	December 10, 2003
Eurex DJEST50	Euro STOXX 50 Index Futures	December 10, 2003
CME MINI S&P	E-mini S&P 500 Futures	December 12, 2003
CME MINI NSDQ	E-mini NASDAQ 100 Futures	September 14, 2004
CME CMX GLD	Gold Futures	July 7, 2005
CME CMX SIL	Silver Futures	July 7, 2005
CME PH CRDE	Crude Oil Futures	November 29, 2004
CME PH NG	Natural Gas (Henry Hub) Physical Futures	November 29, 2004
CME_CBT 30Y TB	U.S. Treasury Bond Futures	October 18, 2004
ICE_NYBOT MNRUS2K	Russell 2000 Index Futures	September 20, 2004
Forex EUR-USD	EUR-USD	July 17, 2009
Forex JPY-USD	JPY-USD	July 17, 2009
Forex GBP-USD	GBP-USD	July 17, 2009
Forex CHF-USD	CHF-USD	July 17, 2009

Table 1: Examined markets and the period of time of the used candle data of the 60 min chart (terminal date is always May 15, 2014). All historical data are from FIDES.

4.2 Results

Now we look at the results for several futures, indexes and foreign exchanges. The statistical quantities for the phase shift of the extreme values are shown in Table 2 and for the points in time of the confirmation of the extreme values in Table 3. The corresponding empirical distributions are given, according to the following remark, by Figures 4 to 20.

Remark 5. *(Notes on figures)*
The label of each of the following figures states "A versus B" and each figure shows the following four distributions (in same order):

1. *Time of extrema: A as primary and B as secondary market.*
2. *Time of extrema: B as primary and A as secondary market.*
3. *Time of extrema confirmed (see Remark 4): A as primary and B as secondary market.*
4. *Time of extrema confirmed (see Remark 4): B as primary and A as secondary market.*

All plots also contains the mean angular direction and the mean angular direction of the weighted distribution (weighted with the hat function, see Figure 3). These directions are the green and red line inside the circle, respectively.

Additionally each bin of the histograms contains information of the single distributions for each wavelength: It shows the largest value of this bin occurred within the 151 *single distributions, the smallest value and the bin value of the combined distribution plus and minus the standard deviation.*

First we discuss the results for the time of extrema and afterwards the results for the confirmation time of the extrema.

prime	sec	$\hat{\alpha} \pm d$	$\hat{\alpha}^{(w)} \pm d^{(w)}$	$\ell^{(w)} \pm d_\ell^{(w)}$/min	$\hat{S}$	$\hat{b}$	$\hat{k}$	p_{ww}	h_m
Eurex DAX*	CME MINI S&P	0.002 ± 0.008	0.012 ± 0.003	11.833 ± 2.674	0.553	0.028	0.349	1.000	0
CME MINI S&P	Eurex DAX*	0.035 ± 0.006	-0.005 ± 0.002	-4.809 ± 2.001	0.522	-0.084	0.426	1.000	1
Forex EUR-USD	Forex JPY-USD*	-0.286 ± 0.081	-0.044 ± 0.006	-41.693 ± 5.571	0.948	0.071	0.161	0.000	1
Forex JPY-USD*	Forex EUR-USD	0.291 ± 0.072	0.028 ± 0.006	26.967 ± 5.572	0.941	-0.098	0.142	0.000	1
Forex EUR-USD	Forex GBP-USD*	0.002 ± 0.011	-0.010 ± 0.003	-9.381 ± 3.303	0.617	-0.031	0.342	1.000	0
Forex GBP-USD*	Forex EUR-USD	0.025 ± 0.011	0.007 ± 0.004	6.269 ± 3.370	0.637	-0.024	0.341	1.000	1
Forex EUR-USD*	Forex CHF-USD	0.000 ± 0.008	0.005 ± 0.003	4.645 ± 2.672	0.489	0.012	0.513	1.000	0
Forex CHF-USD	Forex EUR-USD*	-0.003 ± 0.008	-0.013 ± 0.003	-12.668 ± 2.724	0.492	-0.036	0.501	1.000	0
Eurex BUND	CME_CBT 30Y TB*	-0.036 ± 0.010	-0.007 ± 0.003	-6.534 ± 3.098	0.613	0.038	0.306	1.000	1
CME_CBT 30Y TB*	Eurex BUND	0.078 ± 0.008	0.012 ± 0.003	11.759 ± 2.565	0.612	-0.099	0.331	1.000	1
CME MINI S&P	CME MINI NSDQ*	-0.022 ± 0.005	-0.009 ± 0.002	-8.670 ± 1.749	0.415	0.029	0.578	1.000	1
CME MINI NSDQ*	CME MINI S&P	0.035 ± 0.005	0.013 ± 0.002	12.253 ± 1.746	0.409	-0.050	0.574	1.000	1
ICE_NYBOT MNRUS2K*	CME MINI S&P	0.019 ± 0.005	0.005 ± 0.002	5.004 ± 1.738	0.393	-0.034	0.596	1.000	1
CME MINI S&P	ICE_NYBOT MNRUS2K*	-0.012 ± 0.005	-0.005 ± 0.002	-4.714 ± 1.709	0.402	0.017	0.604	1.000	1
ICE_NYBOT MNRUS2K	CME MINI NSDQ*	-0.014 ± 0.005	-0.012 ± 0.002	-11.257 ± 1.885	0.464	-0.004	0.542	1.000	1
CME MINI NSDQ*	ICE_NYBOT MNRUS2K	0.024 ± 0.005	0.008 ± 0.002	7.952 ± 1.858	0.466	-0.032	0.528	0.948	1
Eurex DJEST50	Eurex DAX*	0.001 ± 0.005	-0.002 ± 0.002	-2.368 ± 2.052	0.323	-0.012	0.638	1.000	0
Eurex DAX	Eurex DJEST50	-0.007 ± 0.005	-0.001 ± 0.002	-0.999 ± 2.058	0.318	0.016	0.620	1.000	1
CME CMX GLD*	CME CMX SIL	0.040 ± 0.006	0.010 ± 0.002	9.576 ± 2.109	0.498	-0.060	0.468	1.000	1
CME CMX SIL*	CME CMX GLD	0.014 ± 0.006	0.010 ± 0.002	9.559 ± 2.086	0.487	-0.002	0.491	1.000	1
CME CMX GLD*	Forex EUR-USD	0.154 ± 0.022	0.030 ± 0.005	28.393 ± 4.488	0.804	-0.091	0.209	0.861	1
Forex EUR-USD	CME CMX GLD*	-0.116 ± 0.022	-0.044 ± 0.005	-42.000 ± 4.334	0.813	0.027	0.227	0.915	1
CME CMX GLD*	CME MINI S&P	0.067 ± 0.030	0.021 ± 0.004	19.585 ± 3.631	0.892	-0.021	0.248	0.000	1
CME MINI S&P	CME CMX GLD*	0.018 ± 0.027	-0.023 ± 0.004	-22.367 ± 3.573	0.883	-0.051	0.239	0.986	0
CME CMX GLD	Eurex DAX*	-0.031 ± 0.029	-0.022 ± 0.004	-21.402 ± 3.696	0.890	-0.016	0.226	0.005	1
Eurex DAX*	CME CMX GLD	-0.018 ± 0.039	0.006 ± 0.005	5.552 ± 4.967	0.897	0.020	0.165	0.000	0
CME CMX GLD*	CME PH CRDE	0.096 ± 0.016	0.028 ± 0.003	27.069 ± 3.142	0.803	-0.048	0.260	1.000	1
CME PH CRDE	CME CMX GLD*	-0.051 ± 0.014	-0.033 ± 0.003	-31.441 ± 3.153	0.767	-0.008	0.264	0.907	1
CME PH CRDE	Eurex DAX*	-0.042 ± 0.018	-0.035 ± 0.003	-33.130 ± 3.302	0.822	-0.024	0.242	1.000	1
Eurex DAX*	CME PH CRDE	0.098 ± 0.024	0.046 ± 0.005	44.008 ± 4.301	0.842	0.001	0.190	1.000	1
CME PH CRDE	Forex EUR-USD*	-0.114 ± 0.018	-0.059 ± 0.005	-56.518 ± 4.366	0.759	0.008	0.221	1.000	1
Forex EUR-USD*	CME PH CRDE	0.149 ± 0.018	0.064 ± 0.004	61.358 ± 4.162	0.774	-0.033	0.224	1.000	1
CME PH CRDE	CME PH NG*	-0.062 ± 0.025	-0.022 ± 0.004	-20.535 ± 3.643	0.876	0.012	0.209	0.009	1
CME PH NG*	CME PH CRDE	0.082 ± 0.025	0.012 ± 0.004	11.090 ± 3.588	0.872	-0.047	0.217	0.008	1

Table 2: Results on 60 min chart (time of extrema). *This market leads the other one.

prime	sec	$\hat{\alpha} \pm d$	$\hat{\alpha}^{(w)} \pm d^{(w)}$	$\ell^{(w)} \pm d_\ell^{(w)}$/min	$\hat{S}$	$\hat{b}$	$\hat{k}$	p_{ww}	h_m
Eurex DAX	CME MINI S&P*	-0.137 ± 0.008	-0.076 ± 0.003	-72.647 ± 2.722	0.548	0.045	0.325	0.000	1
CME MINI S&P*	Eurex DAX	0.039 ± 0.006	0.008 ± 0.002	8.038 ± 2.041	0.511	-0.053	0.392	0.000	1
Forex EUR-USD	Forex JPY-USD*	-0.572 ± 0.051	-0.082 ± 0.006	-78.478 ± 5.384	0.917	0.166	0.080	0.000	1
Forex JPY-USD*	Forex EUR-USD	0.494 ± 0.047	0.086 ± 0.006	81.842 ± 5.381	0.910	-0.143	0.116	0.000	1
Forex EUR-USD	Forex GBP-USD*	-0.053 ± 0.011	-0.029 ± 0.004	-27.782 ± 3.471	0.622	0.012	0.289	0.000	1
Forex GBP-USD*	Forex EUR-USD	0.053 ± 0.011	0.021 ± 0.004	19.941 ± 3.452	0.615	-0.032	0.290	0.000	1
Forex EUR-USD	Forex CHF-USD*	-0.048 ± 0.007	-0.025 ± 0.003	-24.078 ± 2.669	0.461	0.037	0.493	0.002	1
Forex CHF-USD*	Forex EUR-USD	0.065 ± 0.007	0.033 ± 0.003	31.507 ± 2.723	0.463	-0.049	0.477	0.000	1
Eurex BUND	CME_CBT 30Y TB	-0.006 ± 0.010	-0.000 ± 0.003	-0.475 ± 3.175	0.609	0.006	0.280	0.000	0
CME_CBT 30Y TB	Eurex BUND*	0.006 ± 0.008	-0.010 ± 0.003	-9.862 ± 2.550	0.588	-0.033	0.330	0.000	0
CME MINI S&P*	CME MINI NSDQ	-0.004 ± 0.005	0.004 ± 0.002	3.956 ± 1.821	0.410	0.024	0.523	0.039	0
CME MINI NSDQ*	CME MINI S&P	0.021 ± 0.004	0.008 ± 0.002	7.532 ± 1.783	0.385	-0.027	0.529	0.150	1
ICE_NYBOT MNRUS2K	CME MINI S&P	0.005 ± 0.004	-0.002 ± 0.002	-1.512 ± 1.807	0.379	-0.016	0.526	0.000	1
CME MINI S&P*	ICE_NYBOT MNRUS2K	0.022 ± 0.005	0.016 ± 0.002	15.427 ± 1.814	0.404	-0.001	0.519	0.000	1
ICE_NYBOT MNRUS2K	CME MINI NSDQ	-0.004 ± 0.005	-0.002 ± 0.002	-1.685 ± 1.967	0.457	0.005	0.479	0.138	0
CME MINI NSDQ*	ICE_NYBOT MNRUS2K	0.037 ± 0.005	0.017 ± 0.002	16.092 ± 1.948	0.457	-0.032	0.457	0.000	1
Eurex DJEST50*	Eurex DAX	0.007 ± 0.005	0.003 ± 0.002	2.908 ± 2.082	0.317	-0.008	0.615	1.000	1
Eurex DAX	Eurex DJEST50	-0.008 ± 0.005	-0.001 ± 0.002	-1.308 ± 2.083	0.318	0.019	0.612	1.000	1
CME CMX GLD*	CME CMX SIL	0.035 ± 0.005	0.021 ± 0.002	20.262 ± 2.045	0.437	-0.018	0.466	0.995	1
CME CMX SIL	CME CMX GLD*	0.002 ± 0.005	-0.004 ± 0.002	-4.123 ± 2.013	0.417	-0.017	0.490	0.013	0
CME CMX GLD*	Forex EUR-USD	0.072 ± 0.019	0.015 ± 0.005	14.315 ± 4.385	0.778	-0.045	0.228	0.178	1
Forex EUR-USD	CME CMX GLD*	-0.090 ± 0.018	-0.023 ± 0.004	-22.335 ± 4.141	0.776	0.050	0.234	0.998	1
CME CMX GLD*	CME MINI S&P	-0.015 ± 0.034	0.008 ± 0.004	7.721 ± 3.904	0.906	0.021	0.200	0.000	0
CME MINI S&P	CME CMX GLD*	-0.002 ± 0.030	-0.018 ± 0.004	-17.374 ± 3.799	0.896	-0.027	0.204	0.000	0
CME CMX GLD	Eurex DAX	-0.072 ± 0.043	0.001 ± 0.004	1.243 ± 4.043	0.926	0.043	0.189	0.000	1
Eurex DAX	CME CMX GLD*	-0.067 ± 0.072	-0.016 ± 0.006	-15.293 ± 5.379	0.944	0.009	0.165	0.000	0
CME CMX GLD*	CME PH CRDE	0.074 ± 0.015	0.030 ± 0.003	28.410 ± 3.197	0.787	-0.018	0.235	0.000	1
CME PH CRDE	CME CMX GLD*	-0.084 ± 0.014	-0.040 ± 0.003	-38.052 ± 3.225	0.762	0.013	0.242	0.000	1
CME PH CRDE	Eurex DAX*	-0.128 ± 0.018	-0.042 ± 0.004	-40.272 ± 3.367	0.823	0.040	0.225	0.147	1
Eurex DAX	CME PH CRDE	0.038 ± 0.022	0.002 ± 0.005	2.370 ± 4.313	0.830	-0.027	0.172	0.000	1
CME PH CRDE	Forex EUR-USD*	-0.157 ± 0.018	-0.074 ± 0.005	-70.513 ± 4.453	0.765	0.021	0.216	1.000	1
Forex EUR-USD*	CME PH CRDE	0.179 ± 0.019	0.074 ± 0.004	70.949 ± 4.291	0.789	-0.039	0.219	0.989	1
CME PH CRDE	CME PH NG*	-0.171 ± 0.027	-0.035 ± 0.004	-33.655 ± 3.786	0.882	0.059	0.180	1.000	1
CME PH NG*	CME PH CRDE	0.204 ± 0.024	0.041 ± 0.004	39.363 ± 3.698	0.871	-0.078	0.183	0.737	1

Table 3: Results on 60 min chart (time of extrema confirmed). *This market leads the other one.

Time of extrema First we note that the results are mostly independent of the mean wavelength which we can see from the additional information of each bin, i.e. the minimal and maximal value for this bin and the standard deviation. Next we see a very weak correlation between EUR-USD vs. JPY-USD, Gold vs. EUR-USD, Gold vs. S&P 500, Gold vs. FDAX, Gold vs. Oil, Oil vs. FDAX and Oil vs. EUR-USD. The pairs of markets also have a relatively large standard deviation $\hat{S}$ and small concentration around its mean indicated by the small kurtosis $\hat{k}$.

All other combinations of markets illustrated in Table 2 and Figures 4 and 6 to 13 show a large peak near the mean angular direction between 20 % up to 53 %. This means that the probability is significantly high that extreme values for both markets are shaped in almost the exact time. Of course this leads to smaller standard deviations and higher kurtosis.

Confirmation time of extrema Since the point in time of confirming an extreme value by the MinMax process is more sensitive to the price development than the very fixed point in time of the extreme value itself we already expect scattered observations. However even here we can see a peak in the mean angular direction of about half of the size of the peak for the time of extrema of the strongly correlated pairs of markets. The values in Table 3 are approximately of the same order as in Table 2.

All together We see strong correlations for extrema and confirmed extrema between combinations of FDAX, Euro-Bund, Euro STOXX, S&P 500, U.S. Treasury, NASDAQ 100, Russel 2000 and between the foreign exchanges except EUR-USD versus JPY-USD. Additionally Gold and Silver has a strong correlation whereas all other combinations with at least one market from commodities seem to be weakly correlated or even nearly uncorrelated. Thus from the point of view of local extreme values the commodities are separated from other markets.

The lead-lag $\ell^{(w)}$, see Section 3.3, is between 5 min and 10 min for the point in time of the extrema for the indexes and foreign exchanges and also for Gold versus Silver. Note that this is just a fraction of the duration of one single period of the 60 min chart. Even the points in time of the extrema are just the time stamp of a candle and not the exact time of the extreme value itself, i.e. these points in time have an uncertainty of ± 30 min. Therefore we cannot view the value $\ell^{(w)}$ as an absolute value but more as a tendency of the lead or lag for the candles in which the extreme values occur.

Remark 6. *In most of the cases our investigations of the correlation of two markets yields one market leading and one market following, e.g. DAX Futures leads E-mini S&P 500 Futures, no matter which one is considered primary or secondary market. Note however, that in some cases the leading market is not unique like for instance the Gold Futures versus Silver Futures, or, sometimes our calculation cannot decide which market is leading.*

Remark 7. *For the currency Swiss franc it is more common to analyze USD-CHF instead of CHF-USD as we do in the above discussion. The reason we focus on CHF-USD is to see the positive correlation to EUR-USD and thus to have a more natural interpretation for lead and lag as in Definition 1.*

However, it is also possible to compare (strongly) negative correlated markets as EUR-USD versus USD-CHF. In Figure 21 we see the results for this combination. We expect that

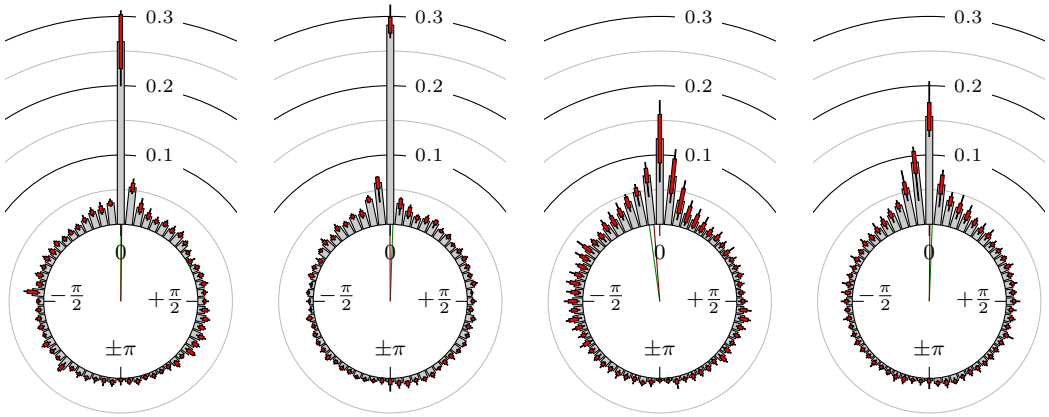

Figure 4: DAX Futures versus E-mini S&P 500 Futures

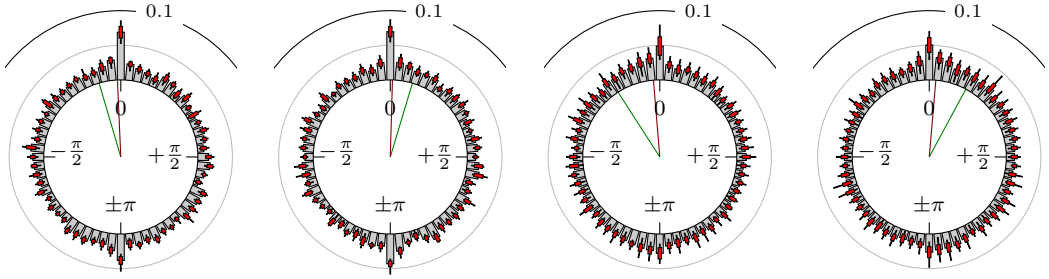

Figure 5: EUR-USD versus JPY-USD

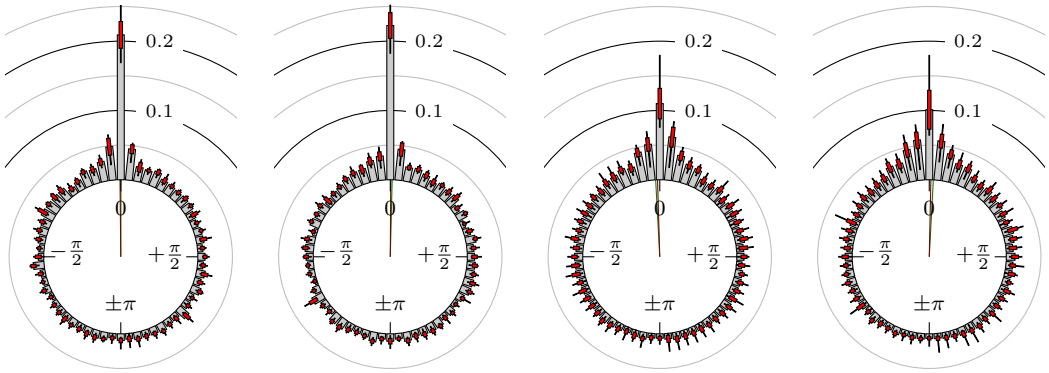

Figure 6: EUR-USD versus GBP-USD

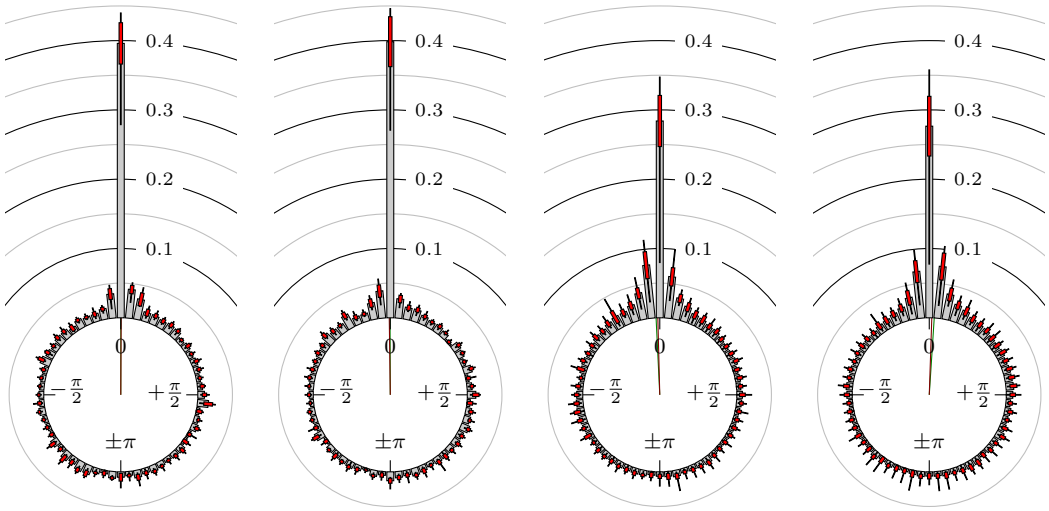

Figure 7: EUR-USD versus CHF-USD

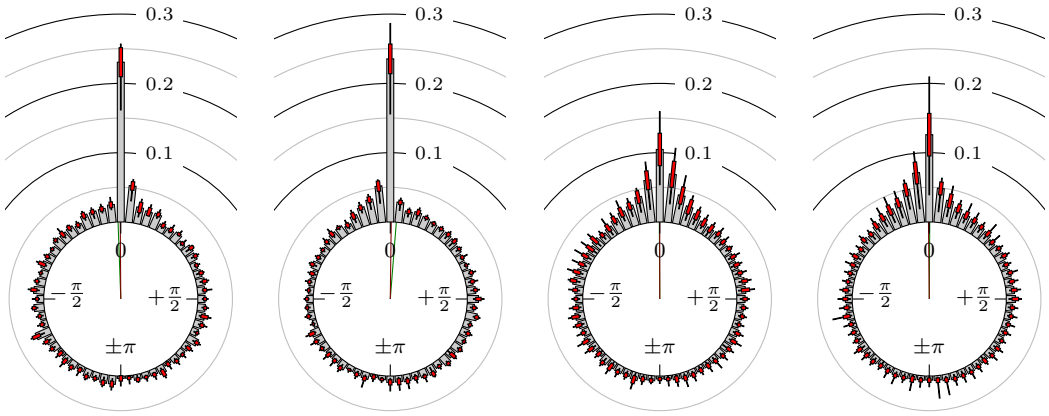

Figure 8: Euro-Bund Futures versus U.S. Treasury Bond Futures

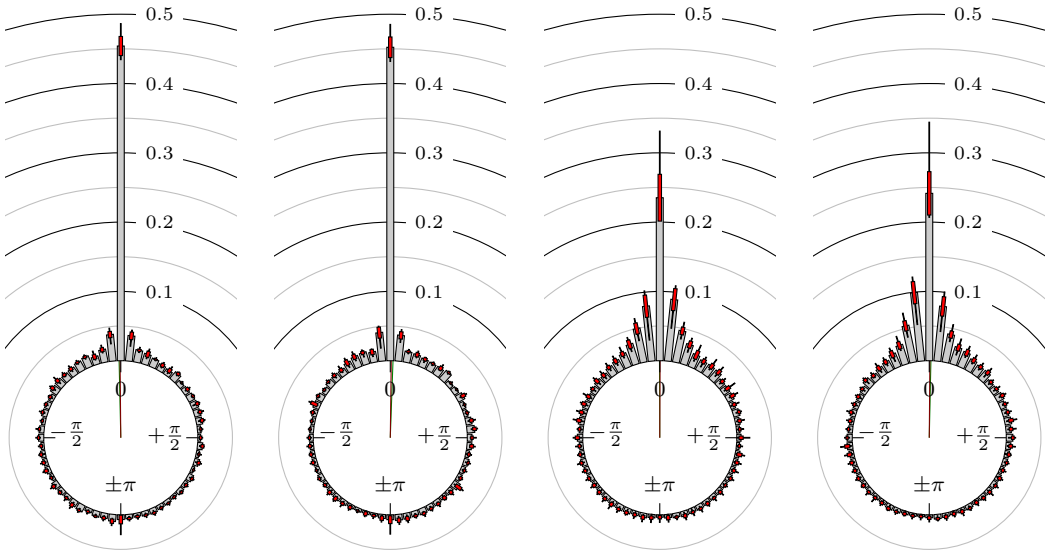

Figure 9: E-mini S&P 500 Futures versus E-mini NASDAQ 100 Futures

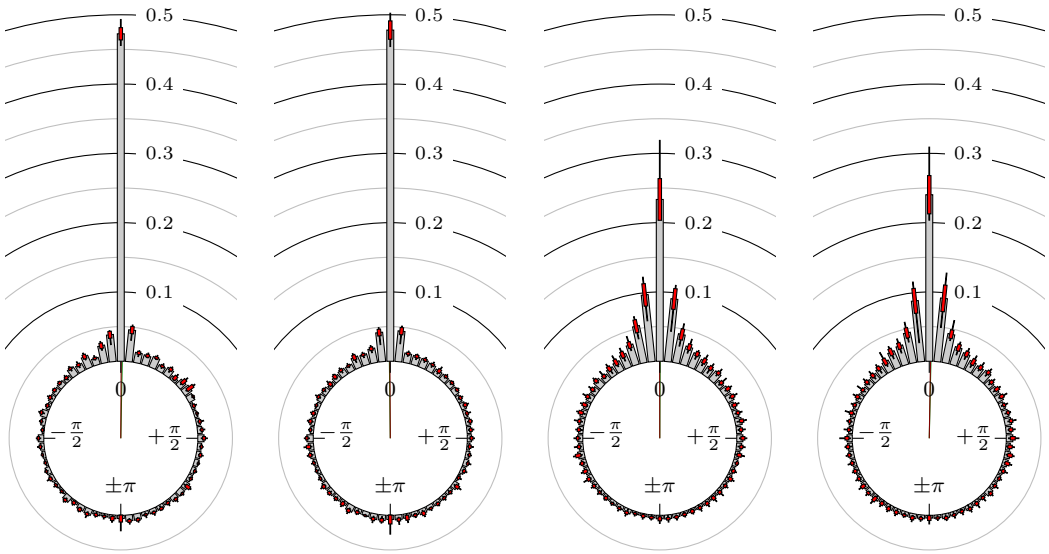

Figure 10: Russell 2000 Index Mini Futures versus E-mini S&P 500 Futures

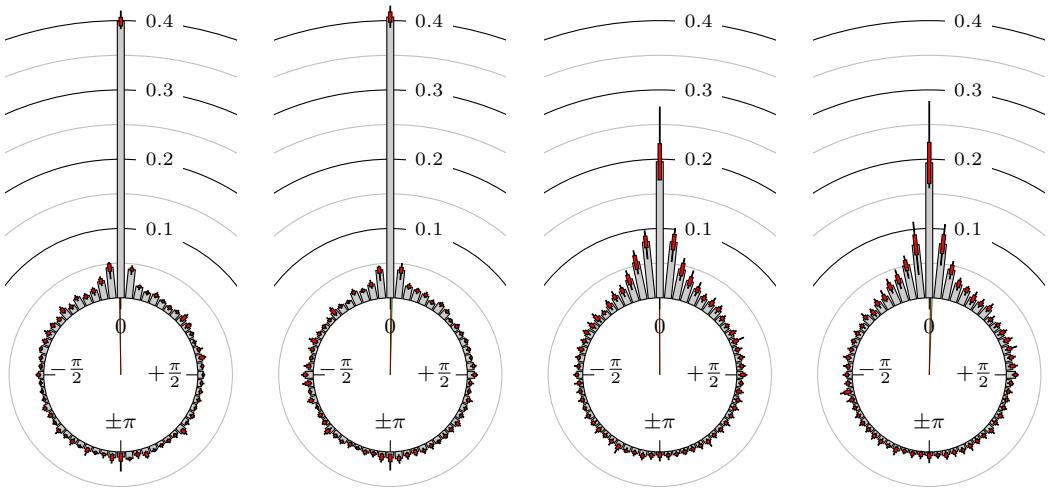

Figure 11: Russell 2000 Index Mini Futures versus E-mini NASDAQ 100 Futures

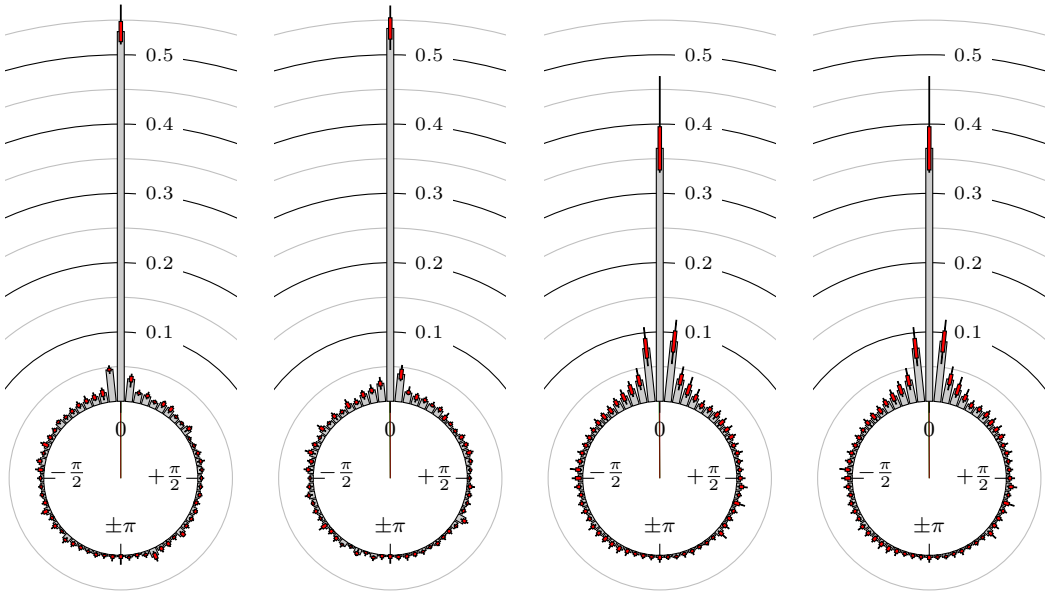

Figure 12: EURO STOXX 50 Index Futures versus DAX Futures

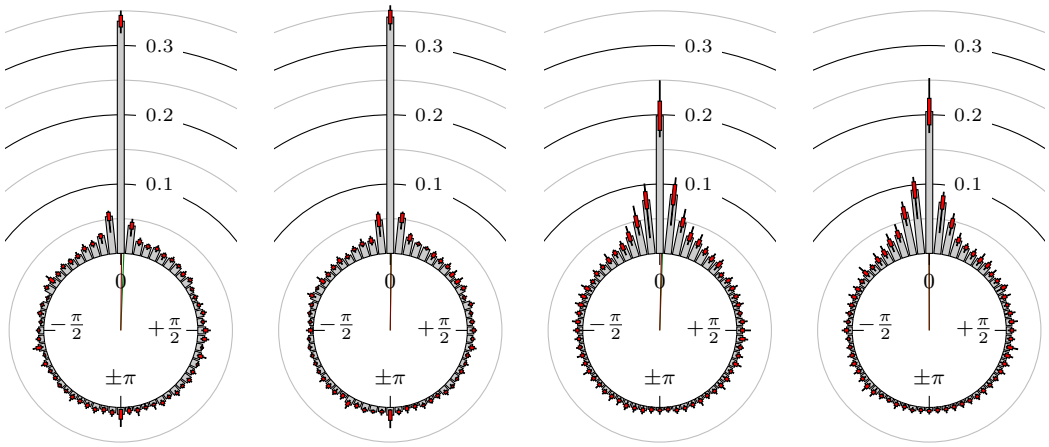

Figure 13: Gold Futures versus Silver Futures

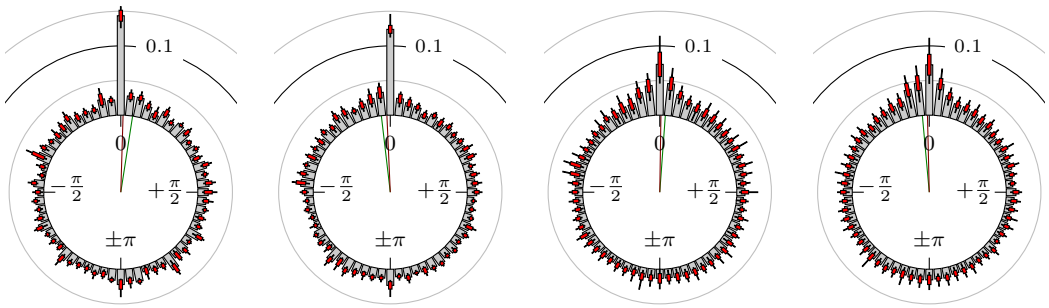

Figure 14: Gold Futures versus EUR-USD

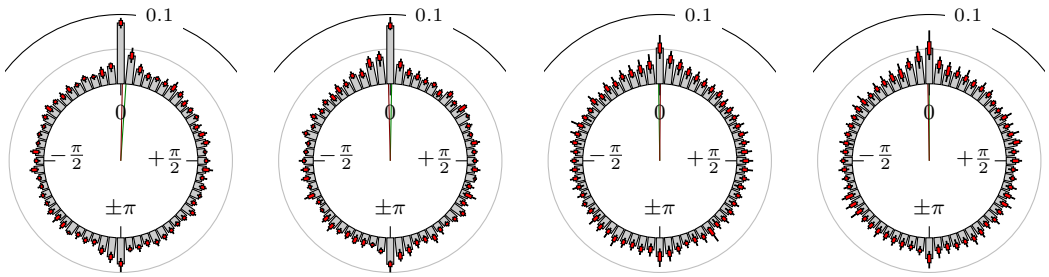

Figure 15: Gold Futures versus E-mini S&P 500 Futures

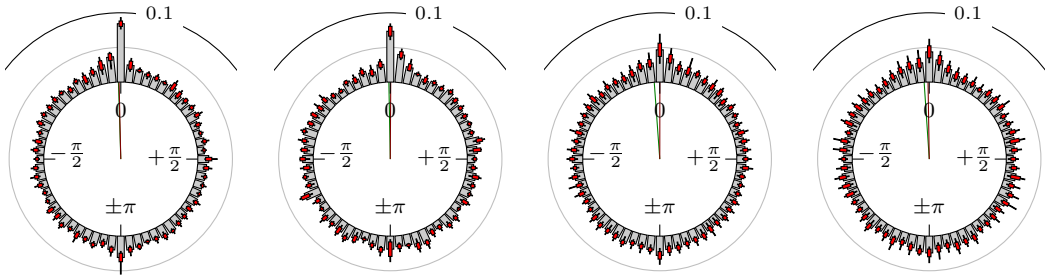

Figure 16: Gold Futures versus DAX Futures

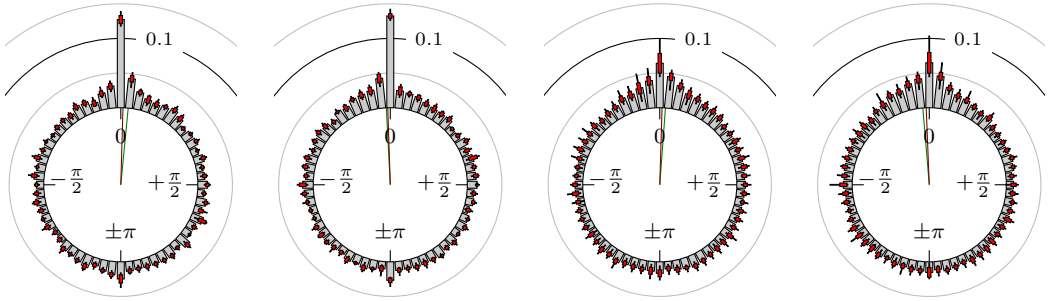

Figure 17: Gold Futures versus Crude Oil Futures

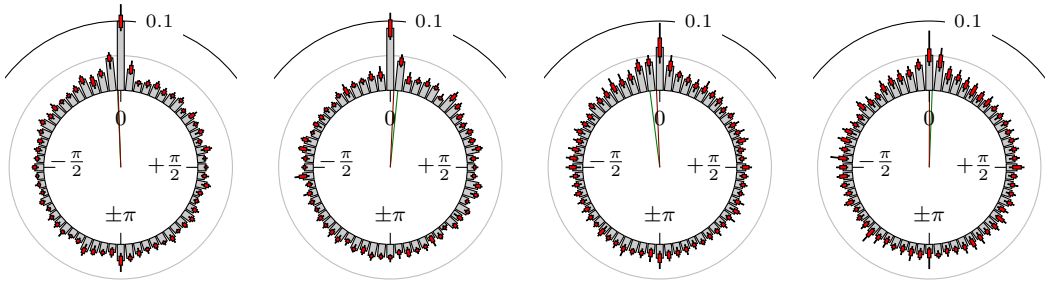

Figure 18: Crude Oil Futures versus DAX Futures

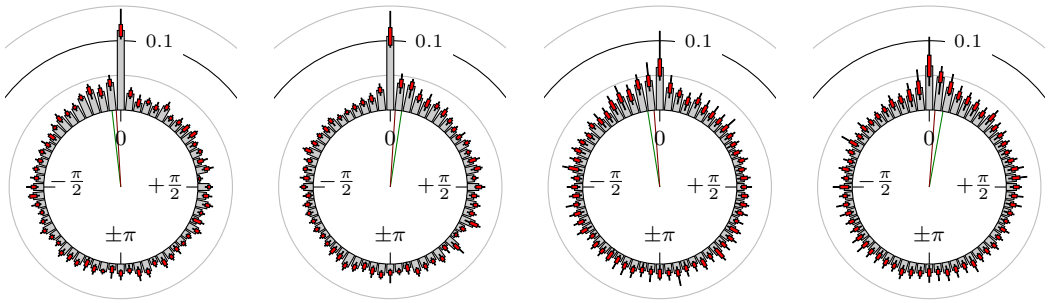

Figure 19: Crude Oil Futures versus EUR-USD

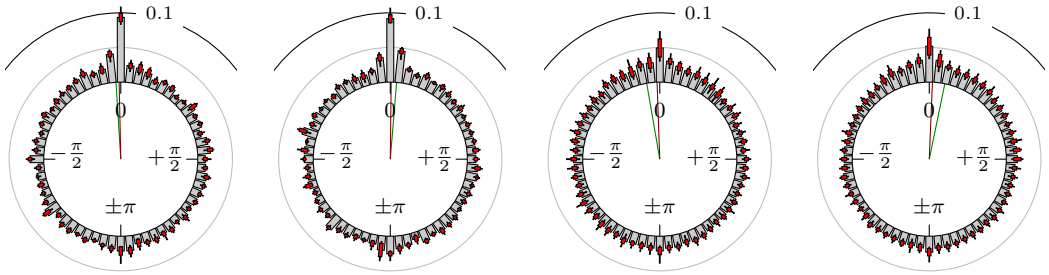

Figure 20: Crude Oil Futures versus Natural Gas (Henry Hub) Physical Futures

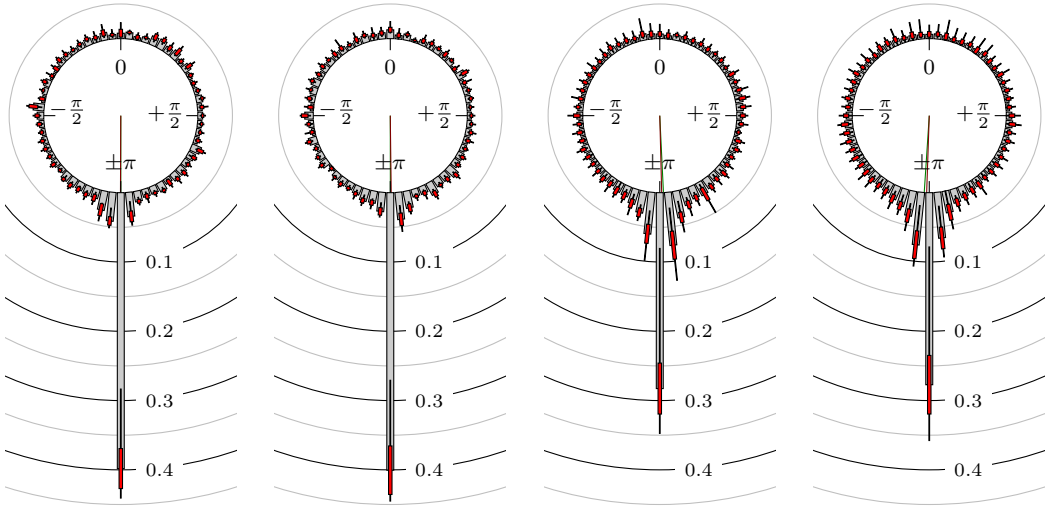

Figure 21: EUR-USD versus USD-CHF (cf. Figure 7)

the results are the same as for the combination EUR-USD versus CHF-USD but shifted by π*. If we compare Figures 7 and 21 we actually see this connection perfectly. This is also the case for the Japanese yen.*

5 Conclusion and outlook

We introduced the notion of lead-lag relationship from a market technical point of view. Using the local extreme values of the markets we get an empirical distribution of their phase shifts on the unit sphere. The directional statistics helps us to illustrate and quantify the results.

We observed many strongly correlated pairs of markets with respect to their extreme values while, of course, there are combinations with a very weak connection. Combinations of indexes show the highest correlation and also a measurable lead or lag. Since we use a geometrical approach based on the actual local extreme values of the chart, i.e. on some kind of reversal points, the results can directly be used for trading strategies.

In future work the authors plan to localize this method to shorter time intervals so that we obtain even more meaningful results for live/real time data.

References

[1] Appel, Gerald: *Technical Analysis: Power Tools for Active Investors.* Financial Times Prentice Hall, Upper Saddle River, NJ, 2005.

[2] Berens, P.: *CircStat: A MATLAB Toolbox for Circular Statistics.* Journal of Statistical Software, 31(10), 2009.

[3] Bollen, J., H. Mao and X. Zeng: *Twitter mood predicts the stock market.* Journal of Computational Science, 2(1):1–8, 2011. DOI: 10.1016/j.jocs.2010.12.007.

[4] Chan, K.: *Imperfect Information and Cross-Autocorrelation Among Stock Prices.* The Journal of Finance, 48(4):1211–1230, 1993. DOI: 10.1111/j.1540-6261.1993.tb04752.x.

[5] Dajčman, S.: *Interdependence Between Some Major European Stock Markets – A Wavelet Lead/Lag Analysis.* Prague Economic Papers, 22(1):28–49, 2013.

[6] de Jong, F. and M. W. M. Donders: *Intraday Lead-Lag Relationships Between the Futures-, Options and Stock Market.* Review of Finance, 1(3):337–359, 1998. DOI: 10.1023/A:1009765322522.

[7] de Jong, F. and T. Nijman: *High frequency analysis of lead-lag relationships between financial markets.* Journal of Empirical Finance, 4(2–3):259–277, 1997. DOI: 10.1016/S0927-5398(97)00009-1.

[8] Didier, T., I. Love and M. D. M. Pería: *What explains comovement in stock market returns during the 2007–2008 crisis?* International Journal of Finance & Economics, 17(2):182–202, 2012. DOI: 10.1002/ijfe.442.

[9] Égert, B. and E. Kočenda: *Time-varying synchronization of European stock markets.* Empirical Economics, 40(2):393–407, 2011. DOI: 10.1007/s00181-010-0341-3.

[10] Fiedor, P.: *Information-theoretic approach to lead-lag effect on financial markets.* The European Physical Journal B, 87:168, 2014. DOI: 10.1140/epjb/e2014-50108-3.

[11] Fisher, N. I.: *Statistical Analysis of Circular Data.* Cambridge University Press, 1996.

[12] Garcia, R. and G. Tsafack: *Dependence structure and extreme comovements in international equity and bond markets.* Journal of Banking & Finance, 35(8):1954–1970, 2011. DOI: 10.1016/j.jbankfin.2011.01.003.

[13] Gençay, R., F. Selçuk and B. Whitcher: *An Introduction to Wavelets and Other Filtering Methods in Finance and Economics.* Academic Press, New York, 2001.

[14] In, F. and S. Kim: *The Hedge Ratio and the Empirical Relationship between the Stock and Futures Markets: A New Approach Using Wavelet Analysis.* The Journal of Business, 79(2):799–820, 2006. DOI: 10.1086/499138.

[15] Iwaisako, T.: *Stock Index Autocorrelation and Cross-autocorrelations of Size-sorted Portfolios in the Japanese Market.* Hitotsubashi Journal of Economics, 48(1):95–112, 2007.

[16] Kim, S. and F. In: *The relationship between stock returns and inflation: new evidence from wavelet analysis.* Journal of Empirical Finance, 12(3):435–444, 2005. DOI: 10.1016/j.jempfin.2004.04.008.

[17] Maier-Paape, S.: *Automatic One Two Three.* Quantitative Finance, 15(2):247–260, 2015. DOI: 10.1080/14697688.2013.814922.

[18] Mao, H., S. Counts and J. Bollen: *Predicting Financial Markets: Comparing Survey, News, Twitter and Search Engine Data.* `http://arxiv.org/abs/1112.1051`, 2011.

[19] Mardia, K. V. and P. E. Jupp: *Directional Statistics.* Wiley series in probability and statistics. Wiley, Hoboken, NJ, 1999.

[20] Murphy, J. J.: *Intermarket Analysis: Profiting from Global Market Relationships.* John Wiley & Sons, Hoboken, 2004.

[21] Ramsey, J. B. and C. Lampart: *The Decomposition of Economic Relationships by Time Scale Using Wavelets: Expenditure and Income.* Studies in Nonlinear Dynamics & Econometrics, 3(1):23–42, 1998. DOI: 10.2202/1558-3708.1039.

[22] Ramsey, J. B. and C. Lampart: *Decomposition of Economic Relationships by Timescale using Wavelets.* Macroeconomic Dynamics, 2(1):49–71, 1998.

[23] Ruggiero, M. A.: *Cybernetic Trading Strategies.* John Wiley & Sons, Hoboken, 1997.

[24] Stoll, H. R. and R. E. Whaley: *The Dynamics of Stock Index and Stock Index Futures Returns.* The Journal of Financial and Quantitative Analysis, 25(4):441–468, 1990. DOI: 10.2307/2331010.

[25] Zar, J. H.: *Biostatistical Analysis.* Pearson, Upper Saddle River, NJ, 5. edition, 2010.

Reports des Instituts für Mathematik der RWTH Aachen

[1] Bemelmans J.: *Die Vorlesung "Figur und Rotation der Himmelskörper" von F. Hausdorff, WS 1895/96, Universität Leipzig*, S 20, März 2005

[2] Wagner A.: *Optimal Shape Problems for Eigenvalues*, S 30, März 2005

[3] Hildebrandt S. and von der Mosel H.: *Conformal representation of surfaces, and Plateau's problem for Cartan functionals*, S 43, Juli 2005

[4] Reiter P.: *All curves in a C^1-neighbourhood of a given embedded curve are isotopic*, S 8, Oktober 2005

[5] Maier-Paape S., Mischaikow K. and Wanner T.: *Structure of the Attractor of the Cahn-Hilliard Equation*, S 68, Oktober 2005

[6] Strzelecki P. and von der Mosel H.: *On rectifiable curves with L^p bounds on global curvature: Self–avoidance, regularity, and minimizing knots*, S 35, Dezember 2005

[7] Bandle C. and Wagner A.: *Optimization problems for weighted Sobolev constants*, S 23, Dezember 2005

[8] Bandle C. and Wagner A.: *Sobolev Constants in Disconnected Domains*, S 9, Januar 2006

[9] McKenna P.J. and Reichel W.: *A priori bounds for semilinear equations and a new class of critical exponents for Lipschitz domains*, S 25, Mai 2006

[10] Bandle C., Below J. v. and Reichel W.: *Positivity and anti-maximum principles for elliptic operators with mixed boundary conditions*, S 32, Mai 2006

[11] Kyed M.: *Travelling Wave Solutions of the Heat Equation in Three Dimensional Cylinders with Non-Linear Dissipation on the Boundary*, S 24, Juli 2006

[12] Blatt S. and Reiter P.: *Does Finite Knot Energy Lead To Differentiability?*, S 30, September 2006

[13] Grunau H.-C., Ould Ahmedou M. and Reichel W.: *The Paneitz equation in hyperbolic space*, S 22, September 2006

[14] Maier-Paape S., Miller U.,Mischaikow K. and Wanner T.: *Rigorous Numerics for the Cahn-Hilliard Equation on the Unit Square*, S 67, Oktober 2006

[15] von der Mosel H. and Winklmann S.: *On weakly harmonic maps from Finsler to Riemannian manifolds*, S 43, November 2006

[16] Hildebrandt S., Maddocks J. H. and von der Mosel H.: *Obstacle problems for elastic rods*, S 21, Januar 2007

[17] Galdi P. Giovanni: *Some Mathematical Properties of the Steady-State Navier-Stokes Problem Past a Three-Dimensional Obstacle*, S 86, Mai 2007

[18] Winter N.: *$W^{2,p}$ and $W^{1,p}$-estimates at the boundary for solutions of fully nonlinear, uniformly elliptic equations*, S 34, Juli 2007

[19] Strzelecki P., Szumańska M. and von der Mosel H.: *A geometric curvature double integral of Menger type for space curves*, S 20, September 2007

[20] Bandle C. and Wagner A.: *Optimization problems for an energy functional with mass constraint revisited*, S 20, März 2008

[21] Reiter P., Felix D., von der Mosel H. and Alt W.: *Energetics and dynamics of global integrals modeling interaction between stiff filaments*, S 38, April 2008

[22] Belloni M. and Wagner A.: *The ∞ Eigenvalue Problem from a Variational Point of View*, S 18, Mai 2008

[23] Galdi P. Giovanni and Kyed M.: *Steady Flow of a Navier-Stokes Liquid Past an Elastic Body*, S 28, Mai 2008

[24] Hildebrandt S. and von der Mosel H.: *Conformal mapping of multiply connected Riemann domains by a variational approach*, S 50, Juli 2008

[25] Blatt S.: *On the Blow-Up Limit for the Radially Symmetric Willmore Flow*, S 23, Juli 2008

[26] Müller F. and Schikorra A.: *Boundary regularity via Uhlenbeck-Rivière decomposition*, S 20, Juli 2008

[27] Blatt S.: *A Lower Bound for the Gromov Distortion of Knotted Submanifolds*, S 26, August 2008

[28] Blatt S.: *Chord-Arc Constants for Submanifolds of Arbitrary Codimension*, S 35, November 2008

[29] Strzelecki P., Szumańska M. and von der Mosel H.: *Regularizing and self-avoidance effects of integral Menger curvature*, S 33, November 2008

[30] Gerlach H. and von der Mosel H.: *Yin-Yang-Kurven lösen ein Packungsproblem*, S 4, Dezember 2008

[31] Buttazzo G. and Wagner A.: *On some Rescaled Shape Optimization Problems*, S 17, März 2009

[32] Gerlach H. and von der Mosel H.: *What are the longest ropes on the unit sphere?*, S 50, März 2009

[33] Schikorra A.: *A Remark on Gauge Transformations and the Moving Frame Method*, S 17, Juni 2009

[34] Blatt S.: *Note on Continuously Differentiable Isotopies*, S 18, August 2009

[35] Knappmann K.: *Die zweite Gebietsvariation für die gebeulte Platte*, S 29, Oktober 2009

[36] Strzelecki P. and von der Mosel H.: *Integral Menger curvature for surfaces*, S 64, November 2009

[37] Maier-Paape S., Imkeller P.: *Investor Psychology Models*, S 30, November 2009

[38] Scholtes S.: *Elastic Catenoids*, S 23, Dezember 2009

[39] Bemelmans J., Galdi G.P. and Kyed M.: *On the Steady Motion of an Elastic Body Moving Freely in a Navier-Stokes Liquid under the Action of a Constant Body Force*, S 67, Dezember 2009

[40] Galdi G.P. and Kyed M.: *Steady-State Navier-Stokes Flows Past a Rotating Body: Leray Solutions are Physically Reasonable*, S 25, Dezember 2009

[41] Galdi G.P. and Kyed M.: *Steady-State Navier-Stokes Flows Around a Rotating Body: Leray Solutions are Physically Reasonable*, S 15, Dezember 2009

[42] Bemelmans J., Galdi G.P. and Kyed M.: *Fluid Flows Around Floating Bodies, I: The Hydrostatic Case*, S 19, Dezember 2009

[43] Schikorra A.: *Regularity of $n/2$-harmonic maps into spheres*, S 91, März 2010

[44] Gerlach H. and von der Mosel H.: *On sphere-filling ropes*, S 15, März 2010

[45] Strzelecki P. and von der Mosel H.: *Tangent-point self-avoidance energies for curves*, S 23, Juni 2010

[46] Schikorra A.: *Regularity of $n/2$-harmonic maps into spheres (short)*, S 36, Juni 2010

[47] Schikorra A.: *A Note on Regularity for the n-dimensional H-System assuming logarithmic higher Integrability*, S 30, Dezember 2010

[48] Bemelmans J.: *Über die Integration der Parabel, die Entdeckung der Kegelschnitte und die Parabel als literarische Figur*, S 14, Januar 2011

[49] Strzelecki P. and von der Mosel H.: *Tangent-point repulsive potentials for a class of non-smooth m-dimensional sets in $\mathbb{R}^n$. Part I: Smoothing and self-avoidance effects*, S 47, Februar 2011

[50] Scholtes S.: *For which positive p is the integral Menger curvature $\mathcal{M}_p$ finite for all simple polygons*, S 9, November 2011

[51] Bemelmans J., Galdi G. P. and Kyed M.: *Fluid Flows Around Rigid Bodies, I: The Hydrostatic Case*, S 32, Dezember 2011

[52] Scholtes S.: *Tangency properties of sets with finite geometric curvature energies*, S 39, Februar 2012

[53] Scholtes S.: *A characterisation of inner product spaces by the maximal circumradius of spheres*, S 8, Februar 2012

[54] Kolasiński S., Strzelecki P. and von der Mosel H.: *Characterizing $W^{2,p}$ submanifolds by p-integrability of global curvatures*, S 44, März 2012

[55] Bemelmans J., Galdi G.P. and Kyed M.: *On the Steady Motion of a Coupled System Solid-Liquid*, S 95, April 2012

[56] Deipenbrock M.: *On the existence of a drag minimizing shape in an incompressible fluid*, S 23, Mai 2012

[57] Strzelecki P., Szumańska M. and von der Mosel H.: *On some knot energies involving Menger curvature*, S 30, September 2012

[58] Overath P. and von der Mosel H.: *Plateau's problem in Finsler 3-space*, S 42, September 2012

[59] Strzelecki P. and von der Mosel H.: *Menger curvature as a knot energy*, S 41, Januar 2013

[60] Strzelecki P. and von der Mosel H.: *How averaged Menger curvatures control regularity and topology of curves and surfaces*, S 13, Februar 2013

[61] Hafizogullari Y., Maier-Paape S. and Platen A.: *Empirical Study of the 1-2-3 Trend Indicator*, S 25, April 2013

[62] Scholtes S.: *On hypersurfaces of positive reach, alternating Steiner formulæ and Hadwiger's Problem*, S 22, April 2013

[63] Bemelmans J., Galdi G.P. and Kyed M.: *Capillary surfaces and floating bodies*, S 16, Mai 2013

[64] Bandle C. and Wagner A.: *Domain derivatives for energy functionals with boundary integrals; optimality and monotonicity.*, S 13, Mai 2013

[65] Bandle C. and Wagner A.: *Second variation of domain functionals and applications to problems with Robin boundary conditions*, S 33, Mai 2013

[66] Maier-Paape S.: *Optimal f and diversification*, S 7, Oktober 2013

[67] Maier-Paape S.: *Existence theorems for optimal fractional trading*, S 9, Oktober 2013

[68] Scholtes S.: *Discrete Möbius Energy*, S 11, November 2013

[69] Bemelmans J.: *Optimale Kurven – über die Anfänge der Variationsrechnung*, S 22, Dezember 2013

[70] Scholtes S.: *Discrete Thickness*, S 12, Februar 2014

[71] Bandle C. and Wagner A.: *Isoperimetric inequalities for the principal eigenvalue of a membrane and the energy of problems with Robin boundary conditions.*, S 12, März 2014

[72] Overath P. and von der Mosel H.: *On minimal immersions in Finsler space.*, S 26, April 2014

[73] Bandle C. and Wagner A.: *Two Robin boundary value problems with opposite sign.*, S 17, Juni 2014

[74] Knappmann K. and Wagner A.: *Optimality conditions for the buckling of a clamped plate.*, S 23, September 2014

[75] Bemelmans J.: *Über den Einfluß der mathematischen Beschreibung physikalischer Phänomene auf die Reine Mathematik und die These von Wigner*, S 23, September 2014

[76] Havenith T. and Scholtes S.: *Comparing maximal mean values on different scales*, S 4, Januar 2015

[77] Maier-Paape S. and Platen A.: *Backtest of trading systems on candle charts*, S 12, Januar 2015

[78] Kolasínski S., Strzelecki P. and von der Mosel H.: *Compactness and Isotopy Finiteness for Submanifolds with Uniformly Bounded Geometric Curvature Energies*, S 44, April 2015

[79] Maier-Paape S. and Platen A.: *Lead-Lag Relationship using a Stop-and-Reverse-MinMax Process*, S 22, April 2015